

# Effect of Oxygen Addition on the Thermokinetic Properties of CO<sub>2</sub> Chemisorption on Li<sub>2</sub>ZrO<sub>3</sub>

Lorena Martínez-dlCruz and Heriberto Pfeiffer\*<sup>‡</sup>

*Instituto de Investigaciones en Materiales, Universidad Nacional Autónoma de México, Circuito exterior s/n, Cd. Universitaria, Del. Coyoacán, CP 04510, México D.F., Mexico*

Lithium zirconate doped with potassium (K-Li<sub>2</sub>ZrO<sub>3</sub>) was synthesized by solid-state reaction and then its CO<sub>2</sub> chemisorption capacity was evaluated using different CO<sub>2</sub>–O<sub>2</sub> gas mixtures. These experiments were performed in order to evaluate the effect produced by the O<sub>2</sub> on the kinetic parameters and on the CO<sub>2</sub> absorption reaction mechanism. Although the CO<sub>2</sub> capture dynamic experiments did not show significant variations as a function of the O<sub>2</sub> content, isothermal experiments and their fitting to the Eyring's model did. Different enthalpy activation ( $\Delta H^\ddagger$ ) values were estimated for the CO<sub>2</sub> chemisorption process, as CO<sub>2</sub> capture is produced by two processes: Initially, the CO<sub>2</sub> chemisorption occurs directly over the K-Li<sub>2</sub>ZrO<sub>3</sub> surface. Then, once a Li<sub>2</sub>CO<sub>3</sub>–ZrO<sub>2</sub> external shell is produced, CO<sub>2</sub> chemisorption is kinetically controlled by diffusion processes, which must imply the lithium and oxygen diffusion. The  $\Delta H^\ddagger$  values, of the CO<sub>2</sub> direct chemisorption, increased as a function of the O<sub>2</sub> content. It was explained in terms of a CO<sub>2</sub>–O<sub>2</sub> competition to occupy the Li<sub>2</sub>ZrO<sub>3</sub> surface. On the other hand, the  $\Delta H^\ddagger$  values, of the CO<sub>2</sub> chemisorption kinetically controlled by diffusion processes, decreased as a function of the O<sub>2</sub> content. This result confirmed the oxygen diffusion dependency of the CO<sub>2</sub> chemisorption on lithium zirconate.

## Introduction

Since 1998, when Nakagawa and Ohashi published a paper,<sup>1</sup> in which it was shown that monoclinic lithium metazirconate (*m*-Li<sub>2</sub>ZrO<sub>3</sub>) was able to trap carbon dioxide (CO<sub>2</sub>), several works have been focused on this ceramic,<sup>2–9</sup> or other lithium ceramics<sup>10–16</sup> as CO<sub>2</sub> captors.

*m*-Li<sub>2</sub>ZrO<sub>3</sub> captures CO<sub>2</sub>, chemically, at high temperatures (reaction 1), producing lithium carbonate (Li<sub>2</sub>CO<sub>3</sub>) and zirconium oxide (ZrO<sub>2</sub>). An advantage of this system is the fact that reaction is reversible; in other words, Li<sub>2</sub>ZrO<sub>3</sub> can be regenerated.



After the initial publication mentioned above, the same and other authors showed that the CO<sub>2</sub> chemisorption process can be importantly improved if the ceramic is doped with potassium (K-doped Li<sub>2</sub>ZrO<sub>3</sub>).<sup>2–5,9</sup> All the papers explained this behavior due to CO<sub>2</sub> diffusion through a molten lithium–potassium carbonate. Later, it was shown a different way to increase the CO<sub>2</sub> chemisorption on the Li<sub>2</sub>ZrO<sub>3</sub>. Ochoa-Fernández et al. showed that the tetragonal phase, *t*-Li<sub>2</sub>ZrO<sub>3</sub>, is much more reactive than the monoclinic phase, as a CO<sub>2</sub> captor.<sup>6–8</sup>

In both cases, as in other lithium ceramics where CO<sub>2</sub> capture occurs chemically, the reaction mechanism proposed is described as follows. Initially, the Li<sub>2</sub>ZrO<sub>3</sub> particles react with CO<sub>2</sub> only at the surface. This superficial reaction involves the formation of a Li<sub>2</sub>CO<sub>3</sub>–ZrO<sub>2</sub> external shell. Then, in order to continue the CO<sub>2</sub> chemisorption on the ceramic, bulk diffusion processes must be activated.<sup>3,4,10,16</sup> From this specific step, the diffusion process, there are several points that have not been totally clarified and understood. Some authors propose that CO<sub>2</sub> diffuse into the ceramic material, while other authors propose a lithium diffusion mechanism. However, none of these theories have been totally proved. Additionally, something else has to be pointed

out from the CO<sub>2</sub> chemisorption reaction on Li<sub>2</sub>ZrO<sub>3</sub>. Into a saturated CO<sub>2</sub> atmosphere, lithium carbonate formation implies that one of each three oxygen atoms, present originally in the Li<sub>2</sub>ZrO<sub>3</sub> ceramic, must become part of the Li<sub>2</sub>CO<sub>3</sub>. Consequently, oxygen diffusion must be involved as well on the reaction mechanism, and not only lithium and/or CO<sub>2</sub> diffuse.

Therefore, the aim of this work was to elucidate if oxygen addition to the gas flow modifies the thermokinetic properties of the CO<sub>2</sub> capture process on Li<sub>2</sub>ZrO<sub>3</sub>. Li<sub>2</sub>ZrO<sub>3</sub> was chosen as a case of study because this ceramic is one of the most studied ceramics as a CO<sub>2</sub> captor.

## Experimental Section

K-doped lithium zirconate, labeled as K-Li<sub>2</sub>ZrO<sub>3</sub>, was synthesized by solid-state reaction, using zirconium oxide (ZrO<sub>2</sub>, Aldrich with 99% purity), lithium carbonate (Li<sub>2</sub>CO<sub>3</sub>, Aldrich with 99+% purity) and potassium carbonate (K<sub>2</sub>CO<sub>3</sub>, Aldrich with 99% purity). The Li<sub>2</sub>CO<sub>3</sub>:ZrO<sub>2</sub>:K<sub>2</sub>CO<sub>3</sub> molar ratio was 1.1:1.0:0.2. Powders were mechanically mixed and then fired at 850 °C for 12 h. The sample was characterized by different techniques such as X-ray diffraction (XRD), scanning electron microscopy (SEM), and dynamic and isothermal thermogravimetric analyses (TGA). For the XRD experiments, a diffractometer Bruker AXS D8 Advance was used coupled to a copper anode X-ray tube. The composition of the sample was identified conventionally by the Joint Committee Powder Diffraction Standard (JCPDS) files. SEM micrographs and elemental analyses (energy dispersive X-ray (EDX)) were obtained in a Cambridge Leica Stereoscan 440 microscope. Before the microscope electronic analysis, powders were coated with gold to avoid the lack of conductivity. Finally, different thermal analyses were performed in the Q500HR equipment from TA Instruments, with an autosampler. The K-Li<sub>2</sub>ZrO<sub>3</sub> sample was heat-treated dynamically, with a heating rate of 5 °C/min from room temperature to 670 °C with different gas-mixtures; CO<sub>2</sub> (100 vol %) and three different CO<sub>2</sub>–O<sub>2</sub> mixtures (98–2, 95–5, and 90–10 vol %), using in all the cases a total flow rate of

\* To whom correspondence should be addressed. Tel.: +52 (55) 5622 4627. Fax: +52 (55) 5616 1371. E-mail: pfeiffer@iim.unam.mx.

<sup>‡</sup> Member of the American Chemical Society.

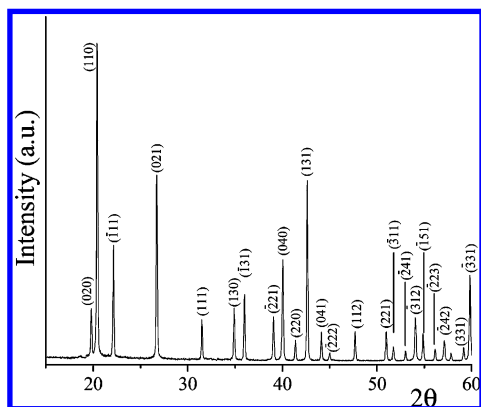


Figure 1. XRD pattern of the K-Li<sub>2</sub>ZrO<sub>3</sub> sample.

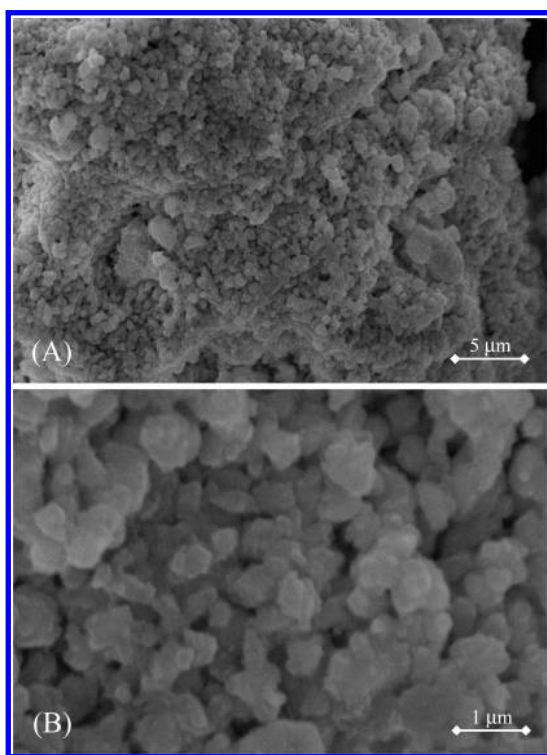


Figure 2. Secondary electron images of the K-Li<sub>2</sub>ZrO<sub>3</sub> sample at two different magnifications.

150 mL/min. Both gases, CO<sub>2</sub> and O<sub>2</sub>, were provided by Praxair with the following grades of purity: 4.0 and 4.8, respectively. Then, the K-Li<sub>2</sub>ZrO<sub>3</sub> sample was tested isothermally at different temperatures, under the same CO<sub>2</sub> and CO<sub>2</sub>-O<sub>2</sub> flows. All the gas mixtures were digitally prepared into a Chem-flow gas mixer from Bel-Japan.

## Results and Discussion

Initially, a K-Li<sub>2</sub>ZrO<sub>3</sub> sample was characterized by different techniques. Figure 1 shows the XRD pattern of the sample. As it can be seen, the XRD pattern fit the 33-0843 JCPDS file, corresponding to the Li<sub>2</sub>ZrO<sub>3</sub> monoclinic phase. Therefore, the presence of potassium in the sample did not produce any kind of structural variation, at least at the XRD detection limits. A second characterization analysis was performed by SEM (Figure 2). The K-Li<sub>2</sub>ZrO<sub>3</sub> sample seemed to be conformed by dense agglomerates of about 20–30 μm, produced by tiny sintered polygonal particles of around 0.5–1 μm (Figure 2A and B). An EDX analysis was performed, in order to verify the presence

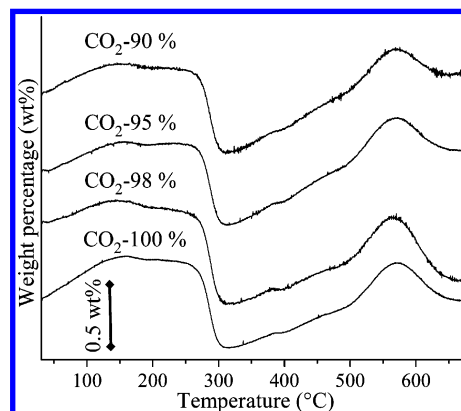


Figure 3. Dynamic thermograms of the K-Li<sub>2</sub>ZrO<sub>3</sub> sample, varying the CO<sub>2</sub>-O<sub>2</sub> gas mixtures from 100 vol % of CO<sub>2</sub> up to 90–10 vol % of CO<sub>2</sub>-O<sub>2</sub>.

of potassium in the K-Li<sub>2</sub>ZrO<sub>3</sub> sample. It has to be taken into account that this analysis is not able to determine lithium and the fact that it is a punctual analysis. Thus, the average Zr and K abundances, on the particle surface, were 15.9 and 0.6 at %, respectively. Although, this result can not be considered as a global elemental analysis, it confirmed the presence of potassium, at least over the surface of the sample. Additionally, SEM morphological results are in total agreement with the synthesis method and heat-treatment utilized.

Once the K-Li<sub>2</sub>ZrO<sub>3</sub> sample was characterized, different dynamic and isothermal analyses were performed, for the CO<sub>2</sub> chemisorption process. These experiments were carried out varying the CO<sub>2</sub>-O<sub>2</sub> volume percentage from 100 vol % of CO<sub>2</sub> to 98–2, 95–5, and 90–10 vol % of CO<sub>2</sub>-O<sub>2</sub>. Dynamic thermogravimetric analyses, varying the CO<sub>2</sub>-O<sub>2</sub> vol %, are presented in Figure 3. As it can be seen, between room temperature and 150 °C, K-Li<sub>2</sub>ZrO<sub>3</sub> gained weight (~0.3–0.4 wt %), independently of the CO<sub>2</sub>-O<sub>2</sub> flow, which may be attributed to a CO<sub>2</sub> capture at the surface of the material. However, it is evident that a sample treated with 100% of CO<sub>2</sub> was the sample that trapped more CO<sub>2</sub>. Once, oxygen was added to the gas flow, the amounts of weight gained decreased. These results suggest a CO<sub>2</sub>-O<sub>2</sub> competition for being initially sorbed over the K-Li<sub>2</sub>ZrO<sub>3</sub> surface. Then, between 150 and 250 °C samples did not present variations on weight. At 250 °C, all the thermograms show a lost of weight, between 0.6 and 0.8 wt % depending on the CO<sub>2</sub>-O<sub>2</sub> molar ratio. These results can be explained by the presence of hydroxyls, as potassium is a highly hygroscopic element, where the superficial hydroxyls formation must be produced during the sample exposition to environment, as an autosampler was used.

The carbonation process was evidenced between 320 and 570 °C. From this part of the thermograms, there is a point that should be mentioned. The weight gained seemed to increase as a function of the oxygen content, as follows: 0.66, 0.66, 0.83, and 0.80 wt % for CO<sub>2</sub>-O<sub>2</sub> volume percentages of 100–0, 98–2, 95–5, and 90–10 vol %, respectively. This result is important as there is a higher absorption even though the oxygen seems to compete with the CO<sub>2</sub> molecules in order to be sorbed over the K-Li<sub>2</sub>ZrO<sub>3</sub> particles. Therefore, it could be proposed that O<sub>2</sub> presence on the gas flow contribute positively to the CO<sub>2</sub> chemisorption. Finally, at higher temperatures than 570 °C all the thermograms showed a lost of weight attributed to the decarbonation process.

In order to further analyze the effect of the oxygen presence on the gas flow, different isothermal experiments were performed on the K-Li<sub>2</sub>ZrO<sub>3</sub> sample (Figure 4). Isotherms with

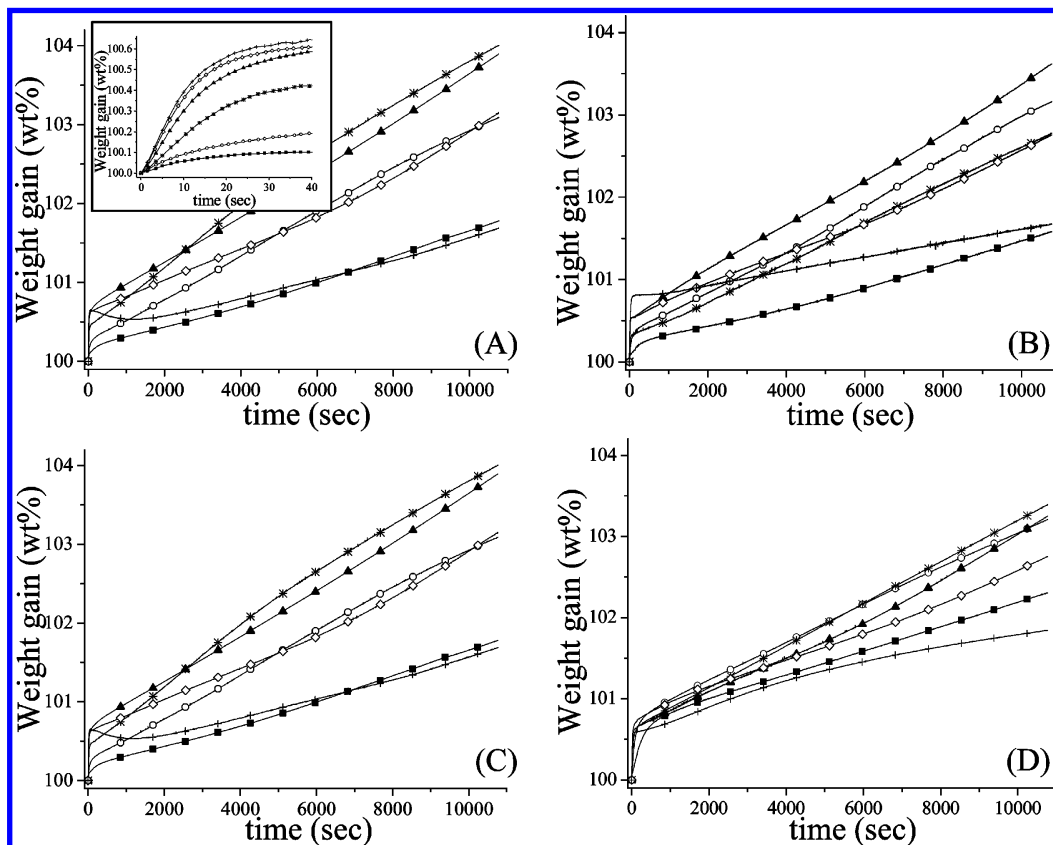


**Figure 4.** Isotherms of the K-Li<sub>2</sub>ZrO<sub>3</sub> sample at different temperatures, varying the CO<sub>2</sub>-O<sub>2</sub> gas mixtures: (A) 100 vol % of CO<sub>2</sub>, (B) 98–2 vol % of CO<sub>2</sub>-O<sub>2</sub>, (C) 95–5 vol % of CO<sub>2</sub>-O<sub>2</sub>, and (D) 90–10 vol % of CO<sub>2</sub>-O<sub>2</sub>. Each temperature was labeled as follows: (■) 420, (○) 440, (\*) 460, (▲) 480, (◇) 500, and (+) 520 °C. The inset in part A corresponds to the first seconds of the same isotherms.

100 vol % of CO<sub>2</sub> are presented in Figure 4A. At short times, the CO<sub>2</sub> chemisorption increased as a function of the isothermal temperature (see inset of Figure 4A), as it could be expected. These results indicate a faster K-Li<sub>2</sub>ZrO<sub>3</sub> surface reactivity when the temperature increases. However, at long times the CO<sub>2</sub> chemisorption behavior varied. Between 420 to 460 °C, the CO<sub>2</sub> chemisorption increased as a function of the temperature, chemisorbing up to 4.0 wt % after 11 000 s at 460 °C. After that, the total CO<sub>2</sub> chemisorption decreased as a function of the temperature. While the sample treated at 480 °C chemisorbed 3.9 wt %, the sample treated at 520 °C only chemisorbed 1.7 wt %. These results suggest that CO<sub>2</sub> desorption is being produced at high temperatures (480–520 °C). Then, at these thermal conditions, K-Li<sub>2</sub>ZrO<sub>3</sub> is chemisorbing CO<sub>2</sub>, but at the same time, the Li<sub>2</sub>CO<sub>3</sub> produced during the CO<sub>2</sub> capture on the first moments of the reaction must decompose and desorb CO<sub>2</sub>. In fact, the desorption process must be slower than the chemisorption process, kinetically, as the isotherm did not reach the equilibrium and their trend is to continue increasing weight.

Similar behaviors were observed on the isotherms performed varying the CO<sub>2</sub>-O<sub>2</sub> vol % as follows: 98–2, 95–5, and 90–10 vol % (Figure 4B–D). In all these cases, the CO<sub>2</sub> chemisorption decrement was detected at 480 °C, as in the previous sample. However, there is an important difference which has to be pointed out: Although the maximum CO<sub>2</sub> chemisorption is always performed at around 460–480 °C, it decreased as a function of the oxygen content, from 4.01 to 3.39 wt %, varying the CO<sub>2</sub>-O<sub>2</sub> flow from 100 to 0 to 90–10 vol %.

For this kind of process, isothermal plots have been usually fitted to double (eq 2) or triple (eq 3) exponential models, as there are two or three different processes taking place. CO<sub>2</sub>

chemisorption is produced under two different conditions: Initially, CO<sub>2</sub> is chemisorbed directly on the K-Li<sub>2</sub>ZrO<sub>3</sub> surface particles (process 1). Then, once the carbonate-oxide external shell is produced, CO<sub>2</sub> chemisorption is kinetically controlled by diffusion processes (process 2). It has to be mentioned that diffusion processes have been usually associated to lithium diffusion from the bulk to the surface of the particles, without taking into account the oxygen requirements. Finally, in those cases where CO<sub>2</sub> desorption process is presented, the triple exponential model was utilized (process 3).<sup>10,16–18</sup>

$$y = A \exp^{-k_1 t} + B \exp^{-k_2 t} + D \quad (2)$$

$$y = A \exp^{-k_1 t} + B \exp^{-k_2 t} - C \exp^{-k_3 t} + D \quad (3)$$

where,  $y$  represents the weight percentage of CO<sub>2</sub> chemisorbed,  $t$  is the time,  $k_1$  is the kinetic constant for the CO<sub>2</sub> direct chemisorption over the Li<sub>2</sub>ZrO<sub>3</sub> particles,  $k_2$  is the kinetic constant for the CO<sub>2</sub> chemisorption kinetically controlled by diffusion processes, and  $k_3$  is the kinetic constant for the CO<sub>2</sub> desorption. Additionally, the pre-exponential factors  $A$ ,  $B$ , and  $C$  indicate the intervals in which each process controls the whole CO<sub>2</sub> chemisorption-desorption process, and the  $D$  constant indicates the  $y$ -intercept.

As it was described qualitatively, all these isothermal experiments fitted to one of these two exponential models and the different constants obtained are presented in the Table 1. From this table, it is evident that CO<sub>2</sub> direct chemisorption constants values ( $k_1$ ) are at least 2 orders of magnitude larger than CO<sub>2</sub> chemisorption kinetically controlled by diffusion processes ( $k_2$ ), in agreement to previous reports.<sup>10,16–18</sup> It means that the second CO<sub>2</sub> chemisorption process is the limiting step. Additionally,

**Table 1. Kinetic Constant Values for the CO<sub>2</sub> Chemisorption Processes and Desorption on K-Li<sub>2</sub>ZrO<sub>3</sub>, Varying Temperature and Using Different CO<sub>2</sub>-O<sub>2</sub> Mixture Gases**

temp (°C)	100 vol % of CO <sub>2</sub>				98 vol % of CO <sub>2</sub>			
	k <sub>1</sub> (1/s)	k <sub>2</sub> (1/s)	K <sub>3</sub> (1/s)	R <sup>2</sup>	k <sub>1</sub> (1/s)	k <sub>2</sub> (1/s)	k <sub>3</sub> (1/s)	R <sup>2</sup>
420	6.0 × 10 <sup>-2</sup>	6.2 × 10 <sup>-6</sup>		0.9154	1.5 × 10 <sup>-2</sup>	6.0 × 10 <sup>-6</sup>		0.9004
440	4.4 × 10 <sup>-2</sup>	4.4 × 10 <sup>-5</sup>		0.9531	2.4 × 10 <sup>-2</sup>	2.2 × 10 <sup>-5</sup>		0.94751
460	5.6 × 10 <sup>-2</sup>	5.3 × 10 <sup>-5</sup>		0.9016	5.5 × 10 <sup>-2</sup>	3.0 × 10 <sup>-5</sup>		0.9356
480	7.0 × 10 <sup>-2</sup>	8.1 × 10 <sup>-5</sup>	7.2 × 10 <sup>-5</sup>	0.9724	7.9 × 10 <sup>-2</sup>	2.7 × 10 <sup>-5</sup>		0.9551
500	9.3 × 10 <sup>-2</sup>	1.1 × 10 <sup>-4</sup>	1.2 × 10 <sup>-4</sup>	0.9822	11.2 × 10 <sup>-2</sup>	4.2 × 10 <sup>-5</sup>	2.6 × 10 <sup>-4</sup>	0.9412
520	9.5 × 10 <sup>-2</sup>	9.8 × 10 <sup>-4</sup>	6.3 × 10 <sup>-5</sup>	0.8421	5.6 × 10 <sup>-2</sup>	6.1 × 10 <sup>-5</sup>	1.1 × 10 <sup>-4</sup>	0.8942
	95 vol % of CO <sub>2</sub>				90 vol % of CO <sub>2</sub>			
420	1.8 × 10 <sup>-3</sup>	4.2 × 10 <sup>-5</sup>		0.9451	4.3 × 10 <sup>-3</sup>	2.4 × 10 <sup>-5</sup>		0.8512
440	2.8 × 10 <sup>-2</sup>	4.5 × 10 <sup>-5</sup>		0.9941	1.2 × 10 <sup>-2</sup>	3.1 × 10 <sup>-5</sup>		0.9014
460	4.4 × 10 <sup>-2</sup>	4.4 × 10 <sup>-5</sup>		0.9415	2.9 × 10 <sup>-2</sup>	3.3 × 10 <sup>-5</sup>		0.9412
480	6.3 × 10 <sup>-2</sup>	3.2 × 10 <sup>-5</sup>		0.9321	5.8 × 10 <sup>-2</sup>	4.3 × 10 <sup>-5</sup>		0.9114
500	5.1 × 10 <sup>-2</sup>	5.4 × 10 <sup>-5</sup>		0.9005	6.3 × 10 <sup>-2</sup>	4.4 × 10 <sup>-5</sup>	1.7 × 10 <sup>-4</sup>	0.8873
520	6.1 × 10 <sup>-2</sup>	8.7 × 10 <sup>-5</sup>	8.1 × 10 <sup>-3</sup>	0.8745	10.5 × 10 <sup>-2</sup>	7.8 × 10 <sup>-5</sup>	4.4 × 10 <sup>-5</sup>	0.9123

the CO<sub>2</sub> desorption constant values ( $k_3$ ) are always smaller than direct CO<sub>2</sub> chemisorption ( $k_1$ ). It confirms the qualitative description given above about the difference on the CO<sub>2</sub> chemisorption and desorption processes. It has to be pointed out that isotherms performed with a CO<sub>2</sub> flow of 100 vol % presented the largest  $k_2$  temperature dependence (Table 1). It may be explained as follows. At this CO<sub>2</sub>-O<sub>2</sub> flow condition, there is not competition between CO<sub>2</sub> and O<sub>2</sub> for being initially sorbed over the K-Li<sub>2</sub>ZrO<sub>3</sub> surface, so CO<sub>2</sub> seemed to be chemisorbed more rapidly; for example, at 420 °C  $k_1$  is at least two times faster with 100 vol % of CO<sub>2</sub> than in any other CO<sub>2</sub>-O<sub>2</sub> flow. Therefore, the results should contribute to a faster activation of the chemisorption kinetically controlled by diffusion processes ( $k_2$ ). In other words, once O<sub>2</sub> was added to the gas flow, CO<sub>2</sub> absorption became slower, even at the K-Li<sub>2</sub>ZrO<sub>3</sub> surface, decreasing the CO<sub>2</sub> chemisorption kinetically controlled by diffusion processes ( $k_2$ ).

In order to completely analyze these data,  $k_1$  and  $k_2$  constant values were fitted to the Eyring's model (eq 4) to elucidate their temperature dependency.

$$\ln(k/T) = -(\Delta H^\ddagger/R)(1/T) + \ln E + \Delta S^\ddagger/R \quad (4)$$

where  $k$  is the rate constant value and  $E$  represents a pre-exponential factor, which in Eyring's formulation is equal to the ratio of Boltzmann's constant to Planck's constant and  $\Delta H^\ddagger$  and  $\Delta S^\ddagger$  are the activation enthalpy and entropy, respectively.

The effect of temperature on the rate constants of CO<sub>2</sub> direct chemisorption and CO<sub>2</sub> chemisorption kinetically controlled by diffusion processes, varying the CO<sub>2</sub>-O<sub>2</sub> volume ratio, are illustrated in Figure 5A and B. Fitting these data to linear plots gave the activation enthalpies ( $\Delta H^\ddagger$ ) for the different processes, which are plotted, as well, in the Figure 5C. Initially, when CO<sub>2</sub> chemisorption on K-Li<sub>2</sub>ZrO<sub>3</sub> was performed in a saturated CO<sub>2</sub> atmosphere (CO<sub>2</sub> 100 vol %), the  $\Delta H^\ddagger$  values obtained were 5.8 and 43 kJ/mol for the CO<sub>2</sub> direct chemisorption reaction and CO<sub>2</sub> chemisorption controlled by diffusion processes, respectively. These results clearly show that CO<sub>2</sub> chemisorption controlled by diffusion processes is more dependent on temperature than CO<sub>2</sub> direct chemisorption. However, when oxygen was added to the CO<sub>2</sub> flow, these tendencies changed notably. For a CO<sub>2</sub>-O<sub>2</sub> flow of 98-2 vol %, the two  $\Delta H^\ddagger$  values became similar: 16.9 and 19.9 kJ/mol for the CO<sub>2</sub> direct chemisorption reaction and the CO<sub>2</sub> chemisorption controlled by diffusion processes, respectively. Here, two different effects were produced, a significant increment of the temperature dependency of the CO<sub>2</sub> direct chemisorption, and perhaps the most important, a decrement of the temperature dependency of the CO<sub>2</sub> chemisorption kinetically controlled by

diffusion processes. The increment of the temperature dependency of the CO<sub>2</sub> direct chemisorption may be explained in terms of CO<sub>2</sub> saturation over the K-Li<sub>2</sub>ZrO<sub>3</sub> surface particles. As there are O<sub>2</sub> molecules present on the gas, they must compete

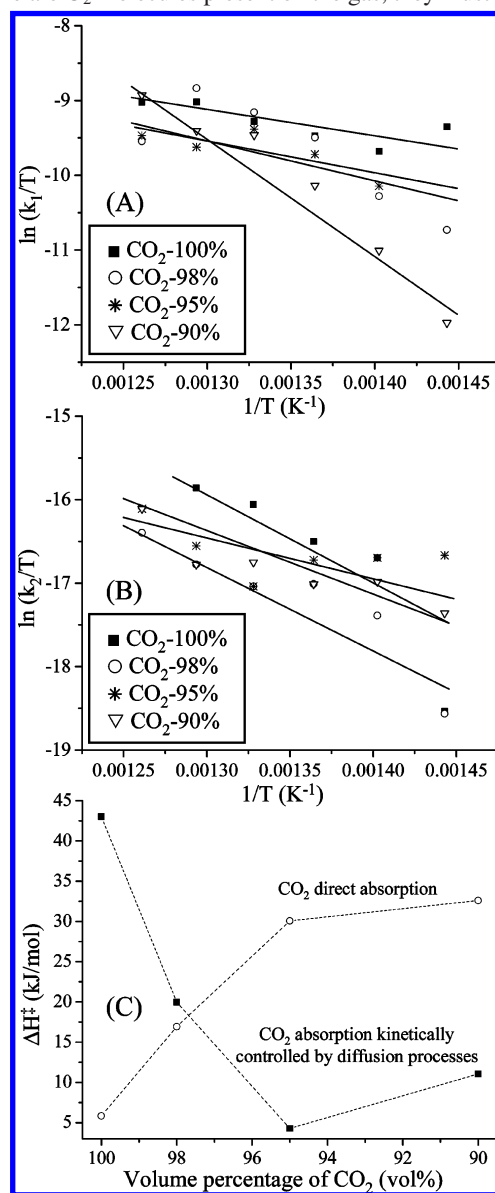


**Figure 5.** Eyring's plots for the rate constant values of the two CO<sub>2</sub> chemisorption processes: direct (A) and kinetically controlled by diffusion processes (B). Plot of the  $\Delta H^\ddagger$  values of both processes as a function of the oxygen content (C).



with the CO<sub>2</sub> molecules for some places on the particle surface. Nevertheless, the most important feature corresponds to the decrement of the temperature dependency of the CO<sub>2</sub> chemisorption kinetically controlled by diffusion processes. In this case, as CO<sub>2</sub> chemisorption is controlled through a bulk process (diffusion), it can not be attributed to the same molecule competition. Therefore, the presence of oxygen must be changing the bulk diffusion process in some way, which is directly correlated to this second CO<sub>2</sub> chemisorption process. The carbonation process implies that two lithium atoms and one oxygen atom, from the Li<sub>2</sub>ZrO<sub>3</sub> crystal, react with CO<sub>2</sub> to produce Li<sub>2</sub>CO<sub>3</sub>. In other words, the diffusion process not only corresponds to the lithium atoms, but one-third of the oxygen atoms as well. In the first moments of the CO<sub>2</sub> chemisorption, there are lithium and oxygen atoms on the Li<sub>2</sub>ZrO<sub>3</sub> surface, and then reaction occurs directly. However, once the carbonate-oxide shell is formed, lithium and oxygen atoms must diffuse, from the bulk to the surface, in order to continue the CO<sub>2</sub> chemisorption. Hence, if the gas flow contains oxygen, its diffusion might be reduced or even not needed. This may explain why this process is not as dependent on temperature as in the previous system reaction. These interpretations were confirmed increasing the oxygen contents to 95–5 and 90–10 vol % of CO<sub>2</sub>–O<sub>2</sub> vol %, respectively. In those cases, while the  $\Delta H^\ddagger$  values of the CO<sub>2</sub> direct chemisorption reaction continued increasing (30.1 and 32.6 kJ/mol for CO<sub>2</sub>–O<sub>2</sub> volume ratios of 95–5 and 90–10 vol %),  $\Delta H^\ddagger$  values of the CO<sub>2</sub> chemisorption controlled by diffusion processes decreased to 4.3 and 11.0 kJ/mol. As it can be seen, in these conditions, the CO<sub>2</sub> direct chemisorption reaction is more dependent on temperature than CO<sub>2</sub> kinetically controlled by diffusion processes.

## Conclusions

CO<sub>2</sub> absorption kinetics, of K-Li<sub>2</sub>ZrO<sub>3</sub> under different CO<sub>2</sub>–O<sub>2</sub> gas flows, was analyzed in this work. First, the sample was prepared by a solid-state reaction and then characterized to obtain composition and morphological properties. Dynamic thermogravimetric experiments, of the CO<sub>2</sub> capture process on different CO<sub>2</sub>–O<sub>2</sub> gas flows, suggested that O<sub>2</sub> addition into the gas mixtures improve the CO<sub>2</sub> chemisorption, when it is kinetically controlled by diffusion processes. Therefore, different isothermal experiments were performed. From the last experiments, it could be said that oxygen addition into the gas flow changes the thermal dependency of the CO<sub>2</sub> chemisorption on K-Li<sub>2</sub>ZrO<sub>3</sub>. It was identified measuring the  $\Delta H^\ddagger$  values. The presence of oxygen produced a reduction of the temperature dependency of the CO<sub>2</sub> chemisorption kinetically controlled by diffusion processes, which involves lithium and oxygen diffusion during the lithium carbonate formation. Conversely, the presence of oxygen over the K-Li<sub>2</sub>ZrO<sub>3</sub> particles partially inhibits the CO<sub>2</sub> chemisorption process, due to a CO<sub>2</sub>–O<sub>2</sub> competition to occupy the Li<sub>2</sub>ZrO<sub>3</sub> surface, so the CO<sub>2</sub> chemisorption reaction becomes more dependent on temperature.

## Acknowledgment

This work was performed in the PUNTA-IMPULSA UNAM framework program and financially supported by CONACYT (23418, 60980), ICyT-DF (179/2009), and PAPIIT-UNAM (IN100609). L.M.-d.C. thanks CONACYT for personal financial support. The authors would like to thank to A. Tejada, O. Novelo, and E. Fregoso for technical help.

## Literature Cited

- (1) Nakagawa, K.; Ohashi, T. A Novel Method of CO<sub>2</sub> capture from high temperature gases. *J. Electrochem. Soc.* **1998**, *145*, 1344.
- (2) Nakagawa, K.; Ohashi, T. A reversible change between lithium zirconate and zirconia in molten carbonate. *Electrochem.* **1999**, *67*, 618.
- (3) Ida, J.; Xiong, R.; Lin, Y. S. Synthesis and CO<sub>2</sub> Sorption Properties of Pure and Modified Lithium Zirconate. *Separ. Purif. Tech.* **2004**, *36*, 41.
- (4) Ida, J.; Lin, Y. S. Mechanism of high-temperature CO<sub>2</sub> sorption on lithium zirconate. *Environ. Sci. Technol.* **2003**, *37*, 1999.
- (5) Pannocchia, G.; Puccini, M.; Seggiani, M.; Vitolo, S. Experimental and modeling studies on high-temperature capture of CO<sub>2</sub> using lithium zirconate based sorbents. *Ind. Eng. Chem. Res.* **2007**, *46*, 6696.
- (6) Ochoa-Fernández, E.; Rusten, H. K.; Jakobsen, H. A.; Rønning, M.; Holmen, A.; Chen, D. Sorption enhanced hydrogen production by steam methane reforming using Li<sub>2</sub>ZrO<sub>3</sub> as sorbent: Sorption kinetics and reactor simulation. *Catal. Today* **2005**, *106*, 41.
- (7) Ochoa-Fernández, E.; Rønning, M.; Grande, T.; Chen, D. Nanocrystalline lithium zirconate with improved kinetics for high-temperature CO<sub>2</sub> capture. *Chem. Mater.* **2006**, *18*, 1383.
- (8) Ochoa-Fernández, E.; Rønning, M.; Yu, X.; Grande, T.; Chen, D. Compositional effects of nanocrystalline lithium zirconate on its CO<sub>2</sub> capture properties. *Ind. Eng. Chem. Res.* **2008**, *47*, 434.
- (9) Xiong, R.; Ida, J.; Lin, Y. S. Kinetics of carbon dioxide sorption on potassium-doped lithium zirconate. *Chem. Eng. Sci.* **2003**, *58*, 4377.
- (10) Alcérreca-Corte, I.; Fregoso-Israel, E.; Pfeiffer, H. CO<sub>2</sub> absorption on Na<sub>2</sub>ZrO<sub>3</sub>: A kinetic analysis of the chemisorption and diffusion processes. *J. Phys. Chem. C* **2008**, *112*, 6520.
- (11) Palacios-Romero, L. M.; Lima, E.; Pfeiffer, H. Structural analysis and CO<sub>2</sub> chemisorption study on non-stoichiometric lithium cuprates (Li<sub>2+x</sub>CuO<sub>2+x/2</sub>). *J. Phys. Chem. A* **2009**, *113*, 193.
- (12) Kato, M.; Yoshikawa, S.; Nakagawa, K. Carbon dioxide absorption by lithium orthosilicate in a wide range of temperature and carbon dioxide concentrations. *J. Mater. Sci. Lett.* **2002**, *21*, 485.
- (13) Essaki, K.; Kato, M.; Uemoto, H. Influence of temperature and CO<sub>2</sub> concentration on the CO<sub>2</sub> absorption properties of lithium silicate pellets. *J. Mater. Sci.* **2005**, *18*, 5017.
- (14) Zhao, T.; Ochoa-Fernández, E.; Rønning, M.; Grande, T.; Chen, D. Preparation and high-temperature CO<sub>2</sub> capture properties of nanocrystalline Na<sub>2</sub>ZrO<sub>3</sub>. *Chem. Mater.* **2007**, *19*, 3294.
- (15) Yamaguchi, T.; Niitsuma, T.; Nair, B. N.; Nakagawa, K. Lithium silicate based membranes for high temperature CO<sub>2</sub> separation. *J. Membr. Sci.* **2007**, *294*, 16.
- (16) Ávalos-Rendón, T.; Casa-Madrid, J.; Pfeiffer, H. Thermochemical capture of carbon dioxide on lithium aluminates (LiAlO<sub>2</sub> and Li<sub>5</sub>AlO<sub>4</sub>): A new option for the CO<sub>2</sub> absorption. *J. Phys. Chem. A* **2009**, *113*, 6919.
- (17) Mejia-Trejo, V. L.; Fregoso-Israel, E.; Pfeiffer, H. Textural, structural, and CO<sub>2</sub> chemisorption effects produced on the lithium orthosilicate by its doping with sodium (Li<sub>4-x</sub>Na<sub>x</sub>SiO<sub>4</sub>). *Chem. Mater.* **2008**, *20*, 7171.
- (18) Mosqueda, H. A.; Vazquez, C.; Bosch, P.; Pfeiffer, H. Chemical sorption of carbon dioxide (CO<sub>2</sub>) on lithium oxide (Li<sub>2</sub>O). *Chem. Mater.* **2006**, *18*, 2307.

Received for review March 8, 2010  
 Revised manuscript received July 11, 2010  
 Accepted August 13, 2010

IE1005417